HHS Public Access

Author manuscript

J Surg Res. Author manuscript; available in PMC 2017 May 15.

Published in final edited form as:

J Surg Res. 2016 May 15; 202(2): 372–379. doi:10.1016/j.jss.2016.02.037.

Severe Burn Increased Skeletal Muscle Loss in *mdx* Mutant Mice

Melody R. Saeman, **Kevin DeSpain**, **Ming-Mei Liu**, **Steven E. Wolf**, and **Juquan Song**[*]

Division of Burn/Trauma/Critical Care, Department of Surgery, University of Texas Southwestern Medical Center, Dallas, Texas

Melody R. Saeman: Melody.Saeman@Phhs.org; Kevin DeSpain: Kevin.DeSpain@UTSouthwestern.edu; Ming-Mei Liu: Ming-Mei.Liu@UTSouthwestern.edu; Steven E. Wolf: Steven.Wolf@UTSouthwestern.edu

Abstract

Background—Severe burn causes muscle mass loss and atrophy. The balance between muscle cell death and growth maintains tissue homeostasis. We hypothesize that pre-existing cellular structural defects will exacerbate skeletal muscle mass loss after burn. Using a Duchenne muscular dystrophy (*mdx*) mutant mouse, we investigated whether severe burn caused more damage in skeletal muscle with pre-existing muscle disease.

Methods—The *mdx* mice and wild type mice received 25% total body surface area (TBSA) scald burn. Gastrocnemius, tibialis anterior, and gluteus muscles were obtained at day 1 and 3 after burn. Gastrocnemius muscle function was measured on day 3. Animals without burn served as controls.

Results—Wet tissue weight significantly decreased in tibialis anterior and gluteus in both *mdx* and wild type mice after burn ($p<0.05$). The ratio of muscle-to-body weight decreased in *mdx* mutant mice ($p<0.05$) but not wild type. Isometric force was significantly lower in *mdx* gastrocnemius and this difference persisted after burn ($p<0.05$). Caspase-3 activity increased significantly after burn in both groups, while HMGB1 expression was higher in burn *mdx* mice ($p<0.05$). Proliferating cell nuclear antigen (PCNA) decreased significantly in *mdx* mice ($p<0.05$). Myogenic markers pax7, myoD and myogenin increased after burn in both groups, and were higher in *mdx* mice ($p<0.05$).

Conclusion—More muscle loss occurred in response to severe burn in *mdx* mutant mice. Cell turnover in *mdx* mice after burn is differed from wild type. Although markers of myogenic activation are elevated in *mdx* mutant mice, the underlying muscle pathophysiology is less tolerant of traumatic injury.

[*]Address correspondence to: Juquan Song, Department of Surgery, UT Southwestern Medical Center, Dallas, TX 75390/9160, Tel: 1-214- 648- 2338, Fax: 1- 214- 648- 8420 ; Email: Juquan.Song@UTSouthwestern.edu

Author contributions: Melody R. Saeman (MRS) contributed to data collection and analysis, and manuscript preparation. Kevin DeSpain (KD) and Ming-Mei Liu (MML) assisted with sample processing and data acquisition. Steven E. Wolf (SEW) was integral to the concept and design of the experiment; the critical revision of the manuscript. Juquan Song (JS) involved all parts of work including study concept, experimental design, data analysis, manuscript preparation and final version approval.

Declaration: Authors have no financial or other interests, which may be construed as a conflict of interest.

Keywords

thermal injury; skeletal muscle; cell death; cell proliferation; myogenesis; preexisting muscle disease

1. Introduction

The hyper-metabolic response to severe burn causes muscle loss to exceed muscle gain resulting in a negative net balance of muscle tissue (1). The mechanisms of muscle loss after burn are not completely understood. Severe burn results in increased resting energy expenditure due to elevated stress hormones, production of acute phase proteins, and increased immunologic mediators (2). Prior studies have demonstrated that increased whole body protein turnover, specifically from breakdown of skeletal muscle, provides amino acid substrates for wound healing after burn (3). However, shunting of amino acids to the burn wound cannot account for muscle loss entirely as net protein loss with elevated catabolism is known to persist nine months to one year after burn, well after wound closure (4, 5).

At the molecular level, it has been observed that caspases and the activated ubiquitin-proteasome pathway leads to accelerated degradation of myofibrillar proteins in the acute phase following burn (6). Specifically, the atrophy-related ubiquitin E3 ligases MuRF-1 and atrogin-1 have been noted to have an 8 and 3 fold increase respectively 48 hours after burn (7). E3 ubiquitin ligases and caspases are regulated through the PI3K pathway, a target of IGF-I and insulin (8).

Skeletal muscle damage is not just limited to depletion of proteins. It has been noted by Duan *et al.* that skeletal muscle cell apoptosis is induced on the first day following burn with a peak at 4 days post-injury. Elevation of circulating apoptotic ligands and caspases as well as an increase in muscle tissue pro-apoptotic genes and proteins suggest a mechanism for this finding (9).

To maintain muscle homeostasis, muscle cell regeneration must compensate for cell death. Myogenesis after burn is not compensatory to cell loss leading to atrophy (10). Myogenesis is dependent on muscle progenitor satellite cells. Satellite cells are a small population of quiescent cells found between the sarcolemma and basal lamina. In response to external stimulation, activated satellite cells first proliferate and then differentiate to fuse into new fibers in the process of repair (11).

The role of myogenesis after burn is not clear. Wu *et al.* have observed satellite cell activation in muscles of severe burn rat models (12). However, Duan *et al.* showed that proliferative activity of myoblasts decreased in the tibialis anterior on the first day after burn, suggesting an inhibition of muscle cell growth (13). After burn, several pathways at the hormonal, cellular, and molecular levels control protein turnover, apoptosis, and myogenesis, all contributing to the end result of muscle atrophy.

Human Duchenne's muscular dystrophy (DMD) is a recessive X-chromosome linked muscular dystrophy caused by a mutation in the dystrophin gene. Patients present with

progressive proximal muscle weakness and loss of muscle mass eventually leading to paralysis. Dystrophin is a cytoplasmic protein that links myofilaments and structural proteins to the sarcolemma. *Dmd*^{mdx} mutant mice (*mdx*) lack dystrophin expression and have been extensively used as an animal model for the human muscular disease (14) (15). This rodent model is considered a less severe phenotype of the human disease, possibly due to the presence of a robust regenerative response or increased expression of utrophin and α7β1-integrin, proteins that fulfill the same structural role as dystrophin (16). To our knowledge, there is no information about the response to severe burn in the dystrophin defective *mdx* mouse. We hypothesize that pre-existing cellular structural defects will exacerbate skeletal muscle mass loss after burn resulting in more severe atrophy. The aim of the current study is to investigate whether severe burn causes more damage in skeletal muscle with pre-existing muscle disease.

2. Materials and methods

Adult male C57BL/10ScSn-*Dmd*^{mdx}/J mutant (*mdx*) mice (6 to 8 weeks old) and aged-matched wild type control mice were purchased from Jackson Laboratory (Bar Harbor, ME) and allowed one week acclimation prior to the experiment. Mice were housed in a temperature-controlled room with a 12-hour light/dark cycle and *ad libitum* laboratory chow and water. All animal procedures were approved by the Institutional Animal Care and Use Committee of the University of Texas Southwestern Medical Center following the National Institutes of Health Guide for the Care and Use of Laboratory Animals.

2.1. Burned mice

Mice received 25% total body surface area (TBSA) scald burn under general anesthesia with 1.2% avertin (250mg/kg) injected intraperitoneally (ip). The burn procedure was described in previous study (17). Briefly, shaved mice received 1 ml of 0.9% saline injection subcutaneously along the spinal column. Mice were placed in a mold with an opening to expose a 12.5% TBSA. Mice were then immersed in 97°C water for 10 seconds on the dorsal and 2 seconds on the ventral side to receive a total 25% TBSA full thickness scald burn. Mice received 1ml of Lactated Ringers solution (ip) for resuscitation, and 0.05 mg/kg of buprenorphine SR subcutaneously for analgesia. Sham animals underwent anesthesia and shaving with immersion in room temperature water (25°C). Hindlimb muscles including gastrocnemius, tibialis anterior and gluteus were obtained when mice were euthanized on day 1 and 3 after burn. Muscle tissue was weighed, halved, and either stored in 10% neutral buffered formalin for histological process, or snap frozen in liquid nitrogen for further molecular biological analysis.

2.2. Muscle function test

Isometric contractile properties of the gastrocnemius muscles were measured on day 3 after burn using an ASI muscle level system with dynamic muscle control and analysis software (1305A whole animal system, Aurora Scientific, Inc.). Under anesthesia, the gastrocnemius muscle was gently dissected free of skin, fascia, and surrounding musculature. The Achilles tendon was sutured and attached to the lever arm of a dual mode servo muscle lever system

(model 305c, Aurora Scientific, Inc). The hind limb was secured to the 806D *in-situ* rodent platform. Electrodes were implanted into the distal end of severed sciatic nerve.

The muscle stimulation protocol was followed the previous study (18) with minor modifications. The gastrocnemius was stimulated by the 701C electrical stimulator (Aurora Scientific, Inc.) with a single twitch (0.2 ms impulse duration, 200 Hz frequency, 10 mA), and the muscle was stretched 0.2 mm every 25 seconds to reach the optimal length (Lo), where there was less than 2% change between twitches. The muscle isometric functions twitch (Pt) and tetanic force (Po) were measured afterwards. Muscle Po was obtained with a total 1 second of electric stimulation at 150 Hz with impulse duration of 0.2 ms and 75 pulses per train. Po was measured triplicated with a 2 minute off tension interval.

2.3. Muscle tissue histology

Fixed muscle tissues were paraffin embedded, and sectioned longitudinally through the middle transverse plane. Tissue sections (5 urn) were deparaffinized and rehydrated following the standard Hematoxylin & Eosin (H&E) staining procedure. With a calibrated eyepiece at 10× magnification, total 100 myofibers from 5 random scope views of each muscle tissue were counted by blinded observers. Values of cell size were analyzed by NIH ImageJ software.

2.4. Western blot

Fifty milligrams of frozen muscle tissue were homogenized in 0.5 ml of T-PER tissue protein extraction reagent containing 1x Halt protease and phosphatase inhibitor cocktail (ThermoFisher Scientific, Rockford, IL).The homogenate was centrifuged at 20,000×g for 30 minutes at 4°C and the supernatant was collected. Thirty micrograms of sample protein were analyzed by SDS-PAGE and western blot following the published procedure (19). Band intensities were quantified with the Gene Snap/Gene Tools software (Syngene, Frederick, MD). Glyceraldehyde-3-phosphate dehydrogenase (GAPDH) was utilized as a loading control. All antibodies including High-mobility group box 1 (HMGB1), proliferating cell nuclear antigen (PCNA), and GAPDH antibodies were purchased from (Cell signaling Tech, Danvers, MA). SuperSignal West Pico Chemiluminescent Substrate was purchased from Thermo Scientific Inc., (Rockford, IL).

2.5. Caspase 3 activity assay

The assay was performed as previously described (17). Tissue protein (20 μg) was incubated with 5 mM Z-DEVD-R110 in reaction buffer containing 5 mM PIPES, pH 7.4, 1 mM EDTA, 0.05% Triton, 5 mM DTT for 30 minutes at room temperature. Fluorescent intensity was detected by FLUOstar OPTIMA microplate reader (BMG-LABTECH Inc., Cary, NC) with excitation/emission 485/520nm filters. Caspase-3 activity was quantified as the change in fluorescence per minute per microgram of protein.

2.6. Real time qPCR

RNA extraction and real time qPCR procedures were published previously (20) and briefly described as following: Total RNA was extracted from 25mg of tissue using RNeasy Fibrous tissue mini kit (Qiagen, Valencia, CA). RNA yield was measured by NanoDrop 3300

Fluorospectrometer (Thermo Fisher Scientific Inc, Wilmington, DE). One microgram (1 μg) of RNA sample was utilized for the first reverse transcription step to make the complementary DNA (cDNA) template using High-capacity cDNA Reverse Transcription kits (Applied Biosystems, Foster city, CA). The cDNA template was stored at -20°C prior to the real time PCR procedure.

Real time quantitative PCR (qPCR) was performed with the standard curve method using IQ5 Multicolor real-time PCR system (Bio-Rad Laboratories, Hercules, CA). The cycle set included stage 1 at 50°C for 2 minutes, stage 2 at 95°C for 10 minutes and stage 3 was repeated 40 times at 95°C for 15 seconds, 60°C for 1 minute. Each sample was run in triplicate. FAM labeled TaqMan probes were purchased from Applied Biosystems. *GAPDH* was set as the reference gene. Relative quantitation of target gene expression was evaluated by the $2^{-\Delta\Delta Ct}$ method.

2.7. Statistical analysis

Statistical analysis was performed using one-way analysis of variance (ANOVA) with Bonferroni post hoc test and paired student's t-test where appropriate. All data are presented as mean ± stand error of the mean (SEM). Significance was accepted at $p<0.05$.

Results

The *mdx* mice had greater body weight (26.38 ± 0.31g vs. 23.51 ± 0.21g) at the beginning of the experiment [Figure 1A]. Following thermal injury, body weight changed significantly with a 10% and 8% decrease at day 1 and 3 in the *mdx* mice compared to a 4% change in wild type (WT) at both days ($p<0.05$) [Figure 1B]. The *mdx* mice had low mRNA and protein expression of dystrophin in muscle tissue [Figure 1C,D]. No significant changes of dystrophin expression were observed in either wild type or mdx mice in response to thermal injury. All animals in both groups survived after burn.

We analyzed the wet tissue mass of three muscle types. Tissue wet weight significantly decreased in the tibialis anterior (TA) of all burned animals with a significantly greater loss of TA tissue mass in the *mdx* mice ($p<0.05$) [Figure 2A]. Gastrocnemius tissue weight in non-burn animals was greater in the *mdx* mice, however, gastrocnemius tissue loss was greater in *mdx* mice at day 1 after burn ($p<0.05$) [Figure 2B]. The gluteus mass significantly decreased over 50% in the *mdx* mice at day 1 and remained low on day 3; it did not decrease significantly until day 3 in WT ($p<0.05$) [Figure 2C]. The ratio of tissue to body weight decreased in all three muscle types in *mdx* mice compared to non-burn, and there was a significant decrease compared to WT mice at day 1 and 3 after burn ($p<0.05$) [Figure 2D,E,F]. Isometric muscle function including twitch (Pt) and tetanic force (Po) were significantly lower in the gastrocnemius of *mdx* mice and remained low when normalized to body weight and after burn ($p<0.05$) [Figure 3].

On histological examination of muscle tissue, we identified progressive degeneration and necrosis in the *mdx* mice. H&E staining showed apparent cell damage with immune cell infiltration in the *mdx* mouse muscle tissue. The muscle cells were swollen with a round shape due to tissue edema and the inflammatory response after burn [Figure 4A]. Single

myofiber size increased 1-fold in the gastrocnemius of *mdx* mice on day 1 after burn with a significant increase in myofiber size of burned *mdx* mice compared to WT [Figure 4B].

Caspase 3 activity increased significantly in the gastrocnemius muscle tissue from both burn *mdx* and WT mice ($p<0.05$). There was not a significant difference in caspase-3 observed between the two burn groups at each time point [Figure 4C]. HMGB1, a necrosis marker, was significantly higher in the *mdx* mice in controls ($p<0.05$) [Figure 4D]. Western blot analysis showed that the band intensity ratio of HMGB1 to GAPDH significantly increased in *mdx* mice at day 1 after burn, and quickly dropped below the baseline on day 3 ($p<0.05$); no significant response was observed in burn WT mice.

Western blot data showed that the absorbance ratio of PCNA to GAPDH was 3-fold higher in muscle from *mdx* mice than wild type mice, and after burn, the ratio of PCNA to GAPDH significantly decreased at day 3 in *mdx* mice ($p<0.05$) [Figure 4E].

The mRNA expression of paired box protein pax7, and myogenic regulatory factors (MRFs) including myoD and myogenin, were examined in gastrocnemius with real time qPCR. Myogenin expression was elevated in *mdx* mice compare to WT mice (13.8 ± 1.48 fold change vs. 3.13 ± 0.35 fold change, $p<0.05$). All mRNA expressions of pax7, myoD and myogenin increased in burn *mdx* mice. MyoD and myogenin mRNA expression were significantly higher in burned *mdx* compared to burned WT mice. Myogenin expression was significantly increased in both burn groups on day 3, with a 7-fold increase seen in *mdx* compared to WT mice ($p<0.05$). [Figure 5]

Discussion

Our investigation of the response to burn in the *mdx* mouse, a model of Duchenne's muscular dystrophy, identified a greater inflammatory response, increased muscle damage, increased cell turnover, and increased cell loss accompanied with a stronger but insufficient myogenic response leading to severe muscle atrophy and body mass loss. The *mdx* mutant mouse has a dystrophin genetic defect causing a muscular dystrophy phenotype. The dystrophin associated protein complex connects the cytoskeleton to the extracellular matrix and stabilizes the sarcolemma. Loss of dystrophin causes instability of the plasma membrane. In the current study, we found that while *mdx* mice had greater body weight at baseline, there was a greater loss of muscle and body mass after burn. Our findings of elevated HMGB1 expression and caspase-3 activity in *mdx* mice suggest increased cell death compared to wild type. Myogenic activation was even higher in response to burn evidenced by an increase in the myogenic factors MyoD, Pax7, and myogenin. However, this did not appear to correlate with an increase in proliferation given the decrease in PCNA expression and the severity of muscle atrophy.

Caspase-3 is a conventional apoptotic cascade signal. In this study we observed that caspase-3 activity increased in both mutant and wild type burn groups, indicating that the apoptosis pathway is activated after burn. HMGB1 is a marker that is passively released by damaged and necrotic cells (21) and we found it was elevated following burn in only *mdx* mice. These findings suggest muscle tissue damage was a cause of necrotic cell death in

mdx mutant mice, while apoptosis is a major cell death pathway in both mutant and wild type mice after burn. The underlying structural defect of the *mdx* mouse muscle fiber appears to increase susceptibility to cellular damage in response to a systemic insult.

Proliferating cell nuclear antigen (PCNA), located in the cell nucleus has an increased expression during the DNA synthesis phase of the cell cycle. It functions as a cofactor of DNA polymerase delta and increases DNA strand synthesis. PCNA has been considered a cell proliferation marker in the study of tissue homeostasis for decades (22, 23). In the current study, we found that PCNA decreased after burn in *mdx* mice. This finding suggests an inhibitory phase of muscle cell growth in *mdx* mice right after burn. Although higher levels of myogenic regulatory factors were found, decreased cell proliferation identifies a breakdown in the myogenesis pathway of *mdx* mice after burn. This finding indicates a mechanism of insufficient muscle homeostasis leading to worsening atrophy.

In this study, we did not observe a trend in the wild type expression of PCNA following burn, however, previously we found that PCNA expression increased after burn in wild type gluteus muscle at day 1 (20). The difference in observations is likely due to the power of the individual studies. The etiology of the decrease in PCNA in burn *mdx* mice compared to controls and wild type mice is not known, however disturbances in intracellular calcium and its effects on endoplasmic reticulum (ER) stress could be a possible mechanism for this finding. Our previous work identified increased stress of the ER in relation to calcium signaling after burn (24). ER stress results in the prevention of protein synthesis. It is established that a deficit in dystrophin results in the disturbance of intracellular calcium homeostasis and effects rates of protein synthesis and turnover; it is possible our observations are related to the interaction of these pathways (25).

We found elevation of the myogenic regulatory factors myoD and myogenin in burn *mdx* mice. Of these, myogenin expression was the most prominent after burn. Myogenin is not only related to myogenesis, but also is an inducer of neurogenic muscle atrophy. There is evidence that myogenin is associated with the activated MRUF1 and atrogin-1 ubiquitin pathway (26). It has previously been shown that necrotic and degenerative muscle fibers in *mdx* mice display an over-activation of the ubiquitin-proteasome system (27). Our finding of increasingly elevated myogenin in *mdx* mice after burn could be reflective of the increased ubiquitin-proteasome protein degradation pathway.

The loss of lean body mass after severe burn is associated with poor clinical outcomes, including an increased chance of infection or sepsis and delayed functional recovery (28) (1). We have shown that pre-existing muscle disease worsens the loss of muscle mass after burn. Muscle homeostasis is not just a problem in the burn unit, but also for the patient with a critical illness causing a hypermetabolic state. Moisey *et al.* reported that critically ill elderly patients with sarcopenia are prone to severe complications and higher mortality (29). Thus patients with pre-existing muscle abnormalities should be evaluated critically by clinical healthcare professionals and the muscle condition taken into consideration of their treatment.

In conclusion, we found increased lean muscle loss in response to severe burn in *mdx* mutant mice. Cell turnover in *mdx* mice after burn is differed form wild type. Our investigation has uncovered the importance of structural muscle proteins in the maintenance of muscle homeostasis after severe burn. The current data implies patients with pre-existing muscle disease are less tolerant of traumatic injury and critical illness.

Acknowledgments

This work was supported by funds from the Golden Charity Guild Charles R Baxter, MD Chair; United States Army Medical Research Administration, TATRC, Department of Defense #W81XWH-12-2-0074-01; and the National Institute for General Sciences of the National Institutes of Health #T32GM008593.

References

1. Hart DW, Wolf SE, Chinkes DL, Gore DC, Mlcak RP, et al. Determinants of skeletal muscle catabolism after severe burn. Annals of surgery. 2000; 232:455–465. [PubMed: 10998644]
2. Porter C, Hurren NM, Herndon DN, Borsheim E. Whole body and skeletal muscle protein turnover in recovery from burns. International journal of burns and trauma. 2013; 3:9–17. [PubMed: 23386981]
3. Gore DC, Chinkes DL, Wolf SE, Sanford AP, Herndon DN, et al. Quantification of protein metabolism in vivo for skin, wound, and muscle in severe burn patients. JPEN. Journal of parenteral and enteral nutrition. 2006; 30:331–338. [PubMed: 16804131]
4. Hart DW, Wolf SE, Mlcak R, Chinkes DL, Ramzy PI, et al. Persistence of muscle catabolism after severe burn. Surgery. 2000; 128:312–319. [PubMed: 10923010]
5. Diaz EC, Herndon DN, Lee J, Porter C, Cotter M, et al. Predictors of muscle protein synthesis after severe pediatric burns. The journal of trauma and acute care surgery. 2015; 78:816–822. [PubMed: 25807408]
6. Lecker SH, Solomon V, Mitch WE, Goldberg AL. Muscle protein breakdown and the critical role of the ubiquitin-proteasome pathway in normal and disease states. The Journal of nutrition. 1999; 129:227S–237S. [PubMed: 9915905]
7. Lang CH, Huber D, Frost RA. Burn-induced increase in atrogin-1 and MuRF-1 in skeletal muscle is glucocorticoid independent but downregulated by IGF-I. American journal of physiology Regulatory, integrative and comparative physiology. 2007; 292:R328–336.
8. Pereira C, Murphy K, Jeschke M, Herndon DN. Post burn muscle wasting and the effects of treatments. The international journal of biochemistry & cell biology. 2005; 37:1948–1961. [PubMed: 16109499]
9. Duan H, Chai J, Sheng Z, Yao Y, Yin H, et al. Effect of burn injury on apoptosis and expression of apoptosis-related genes/proteins in skeletal muscles of rats. Apoptosis : an international journal on programmed cell death. 2009; 14:52–65. [PubMed: 19009350]
10. Quintana HT, Bortolin JA, da Silva NT, Ribeiro FA, Liberti EA, et al. Temporal study following burn injury in young rats is associated with skeletal muscle atrophy, inflammation and altered myogenic regulatory factors. Inflammation research : official journal of the European Histamine Research Society … [et al]. 2015; 64:53–62.
11. Hawke TJ, Garry DJ. Myogenic satellite cells: physiology to molecular biology. Journal of applied physiology. 2001; 91:534–551. [PubMed: 11457764]
12. Wu X, Walters TJ, Rathbone CR. Skeletal muscle satellite cell activation following cutaneous burn in rats. Burns : journal of the International Society for Burn Injuries. 2013; 39:736–744. [PubMed: 23146573]
13. Duan HJ, Chai JK, Sheng ZY, Liang LM, Yin HN, et al. Changes in proliferative activity of myoblasts and expression of Akt in skeletal muscle of rats after severe burn injury. Zhonghua wai ke za zhi [Chinese journal of surgery]. 2009; 47:1261–1264. [PubMed: 19781178]

14. Willmann R, Possekel S, Dubach-Powell J, Meier T, Ruegg MA. Mammalian animal models for Duchenne muscular dystrophy. Neuromuscular disorders : NMD. 2009; 19:241–249. [PubMed: 19217290]
15. Sproule DM, Kaufmann P. Therapeutic developments in spinal muscular atrophy. Therapeutic advances in neurological disorders. 2010; 3:173–185. [PubMed: 21179609]
16. McGreevy JW, Hakim CH, McIntosh MA, Duan D. Animal models of Duchenne muscular dystrophy: from basic mechanisms to gene therapy. Dis Model Mech. 2015; 8:195–213. [PubMed: 25740330]
17. Song J, de Libero J, Wolf SE. Hepatic autophagy after severe burn in response to endoplasmic reticulum stress. The Journal of surgical research. 2014; 187:128–133. [PubMed: 24209807]
18. Saeman MR, DeSpain K, Liu MM, Carlson BA, Song J, et al. Effects of exercise on soleus in severe burn and muscle disuse atrophy. The Journal of surgical research. 2015; 198:19–26. [PubMed: 26104324]
19. Song J, Zhang XJ, Boehning D, Brooks NC, Herndon DN, et al. Measurement of Hepatic Protein Fractional Synthetic Rate with Stable Isotope Labeling Technique in Thapsigargin Stressed HepG2 Cells. International journal of biological sciences. 2012; 8:265–271. [PubMed: 22298954]
20. Song J, Saeman MR, De Libero J, Wolf SE. Skeletal Muscle Loss Is Associated with Tnf Mediated Insufficient Skeletal Myogenic Activation after Burn. Shock. 2015
21. Ulloa L. Messmer D High-mobility group box 1 (HMGB1) protein: friend and foe. Cytokine & growth factor reviews. 2006; 17:189–201. [PubMed: 16513409]
22. Song J, Wolf SE, Wu XW, Finnerty CC, Herndon DN, et al. Proximal gut mucosal epithelial homeostasis in aged IL-1 type I receptor knockout mice after starvation. The Journal of surgical research. 2011; 169:209–213. [PubMed: 20605606]
23. Kubben FJ, Peeters-Haesevoets A, Engels LG, Baeten CG, Schutte B, et al. Proliferating cell nuclear antigen (PCNA): a new marker to study human colonic cell proliferation. Gut. 1994; 35:530–535. [PubMed: 7909785]
24. Jeschke MG, Finnerty CC, Herndon DN, Song J, Boehning D, et al. Severe Injury Is Associated With Insulin Resistance, Endoplasmic Reticulum Stress Response, and Unfolded Protein Response. Annals of surgery. 2012; 255:370–378. [PubMed: 22241293]
25. Kamper A, Rodemann HP. Alterations of protein degradation and 2-D protein pattern in muscle cells of MDX and DMD origin. Biochemical and biophysical research communications. 1992; 189:1484–1490. [PubMed: 1482361]
26. Moresi V, Williams AH, Meadows E, Flynn JM, Potthoff MJ, et al. Myogenin and class II HDACs control neurogenic muscle atrophy by inducing E3 ubiquitin ligases. Cell. 2010; 143:35–45. [PubMed: 20887891]
27. Kumamoto T, Fujimoto S, Ito T, Horinouchi H, Ueyama H, et al. Proteasome expression in the skeletal muscles of patients with muscular dystrophy. Acta neuropathologica. 2000; 100:595–602. [PubMed: 11078210]
28. Jeschke MG, Chinkes DL, Finnerty CC, Kulp G, Suman OE, et al. Pathophysiologic response to severe burn injury. Annals of surgery. 2008; 248:387–401. [PubMed: 18791359]
29. Moisey LL, Mourtzakis M, Cotton BA, Premji T, Heyland DK, et al. Skeletal muscle predicts ventilator-free days, ICU-free days, and mortality in elderly ICU patients. Crit Care. 2013; 17:R206. [PubMed: 24050662]

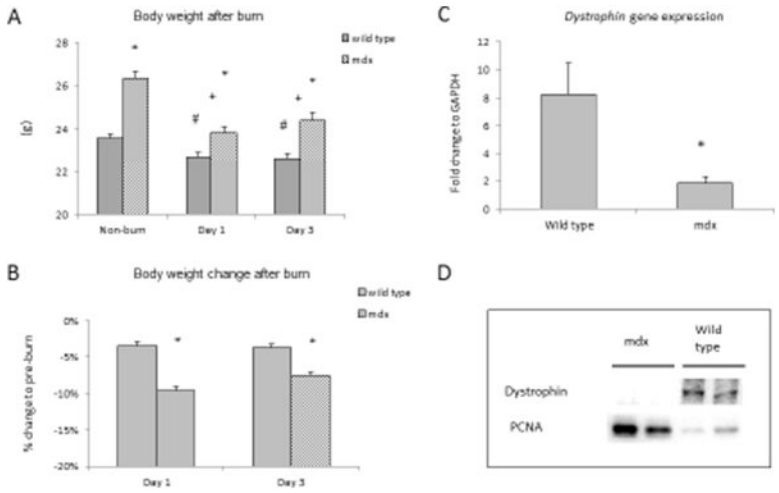

Figure 1.

A) Animal body weight from *mdx* and wild type groups. B) Percentage change of body weight to pre-burn. C) Real time qPCR detected *dystrophin* mRNA expressions, and D) Western blot images showed protein expressions of dystrophin and PCNA from gastrocnemius muscle in sham groups of *mdx* and wild type mice. * $p<0.05$ *mdx* vs. wild type; + $p<0.05$ *mdx* mice vs. non-burn group; # $p<0.05$ wild type vs. non-burn group (n=6/group)

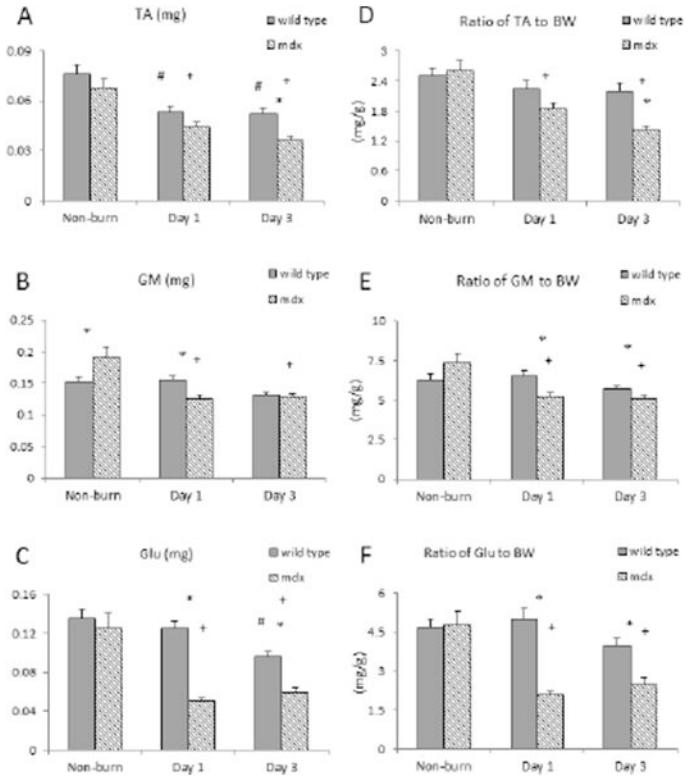

Figure 2.

Tissue weight change after burn. Muscle tissue wet weight alteration of A) tibialis anterior (TA), B) gastrocnemius (GM), and C) gluteus (Glu) in both *mdx* and wild type mice after burn. Normalized muscle tissue wet weight to animals body weight (BW), statistical analysis results of D) the ratio of TA to BW, E) the ratio of GM to BW and F) the ratio of Glu to BW in both *mdx* and wild type mice after burn. * $p<0.05$ *mdx* vs. wild type; + $p<0.05$ *mdx* mice vs. non-burn group; # $p<0.05$ wild type vs. non-burn group (n=6/group)

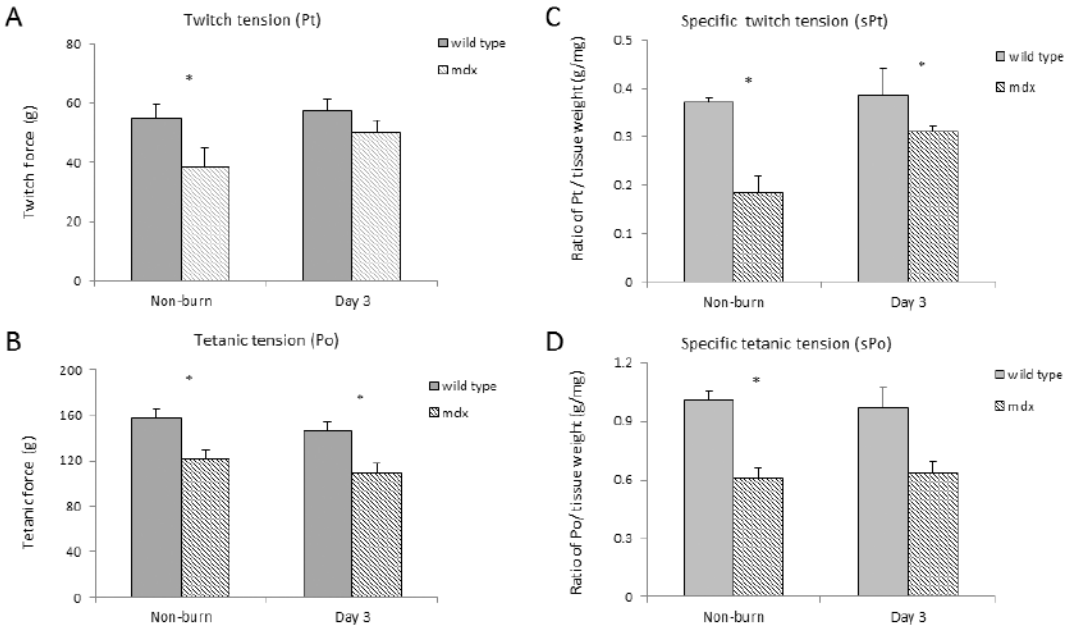

Figure 3.

Muscle isometric force including A) twitch force (Pt), B) tetanic force (Po) at day 3 after burn, C) specific Pt (sPt) and D) specific Po (sPo) forces normalized to tissue weight. * $p<0.05$ *mdx* vs. wild type (n=3/group)

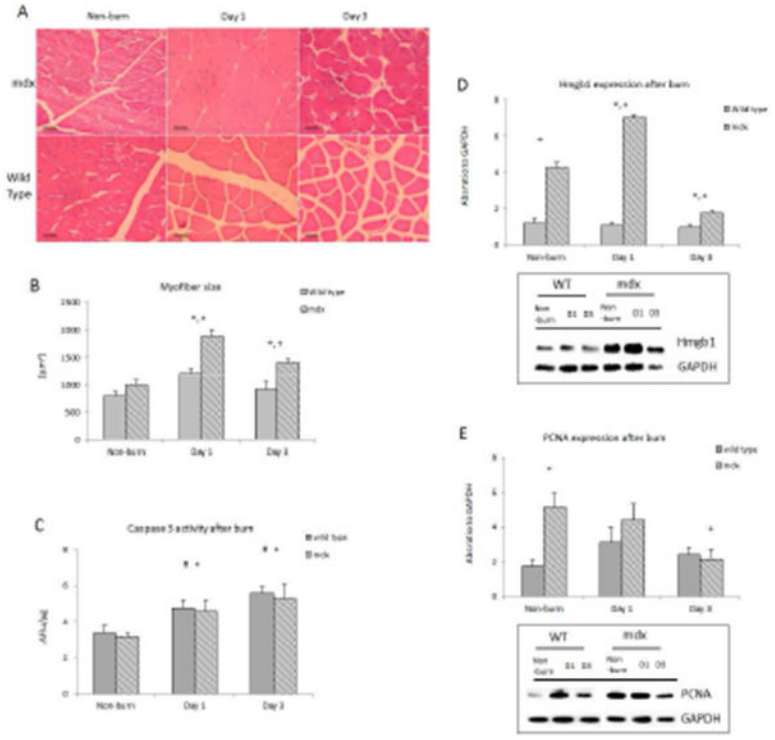

Figure 4.

Muscle histology and cellular homeostasis in response burn. A) Cross sectional tissue slide of mouse gastrocnemius stained with hematoxylin and eosin; B) Myofiber size; C) Caspase-3 activity alterations in both groups after burn; D) HMGB1 western protein expression; E) PCNA protein expression. * $p<0.05$ *mdx* vs. wild type; + $p<0.05$ *mdx* mice vs. non-burn group; # $p<0.05$ wild type vs. non-burn group (n=6/group)

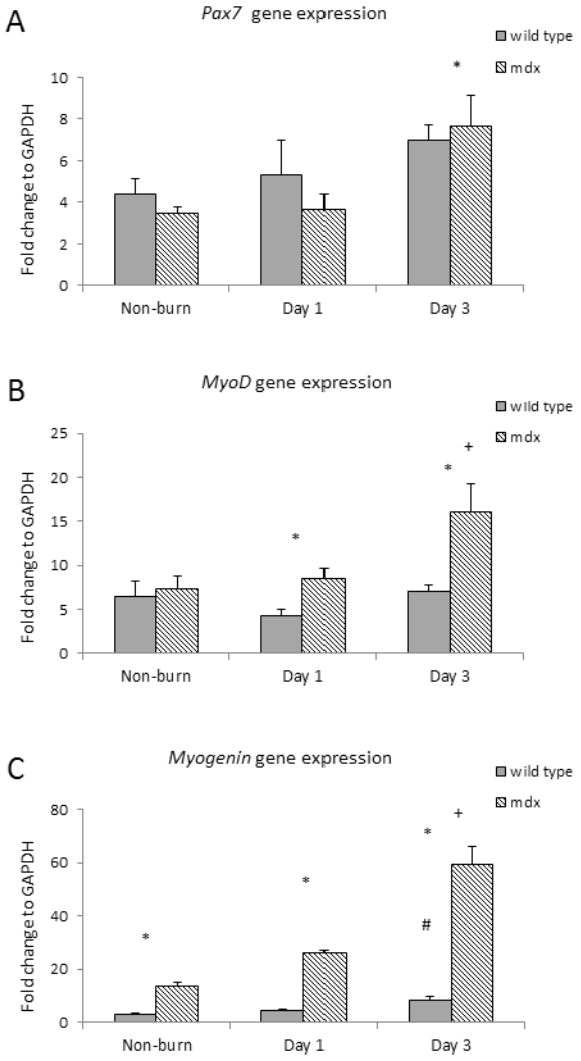

Figure 5.

Myogenic markers A) *Pax7*, B) *MyoD, and* C) *Myogenin* mRNA expression in *mdx* and wild type mice after burn. * $p<0.05$ *mdx* vs. wild type; + $p<0.05$ *mdx* mice vs. non-burn group; # $p<0.05$ wild type vs. non-burn group (n=6/group)